The Proximal Hydrogen-Bonded Residue Controls the Stability of the Compound II Intermediate of Peroxidases and Catalases

Carme Rovira*,† and Ignacio Fita‡

Centre de Recerca en Química Teòrica, Parc Científic de Barcelona, Josep Samitier 1-5, 08028 Barcelona, Spain, and Institut de Biologia Molecular de Barcelona (IBMB-CSIC), Jordi Girona 18-26, 08034 Barcelona, Spain

Received: August 27, 2002; In Final Form: March 14, 2003

The structural and energetic properties of the compound **II** intermediate in the catalytic reaction of peroxidases and catalases are compared in order to investigate why catalases, unlike peroxidases, rarely form compound **II**. Our calculations, based on the density functional theory (DFT)/Car−Parrinello molecular dynamics methodology (CPMD), show that catalase compound **II** is a stable intermediate with respect to ligand dissociation, with Fe−ligand binding energies comparable to those found for other hemeproteins such as myoglobin and cytochrome *c*. Nevertheless, catalase shows much weaker iron−ligand bonds compared to those of peroxidase, which is due to the opposite effect of the proximal hydrogen-bonded residues (Arg^+ in catalase and Asp^- in peroxidase). Comparison with the available structural information suggests that, contrary to the often assumed oxoferryl bond of compound **II**, some of the reported structures might instead correspond to a hydroxyferryl bond. Some hints on the role of the proximal hydrogen-bonded residues in modulating the stability of the different species during the catalytic reaction are provided.

1. Introduction

Heme-based catalases and peroxidases are present in almost all aerobically respiring organisms.[1] Peroxidases oxidize a variety of substrates by reacting first with hydrogen peroxide and catalases protect the cell against the toxic effects of the hydrogen peroxide by decomposing it into molecular oxygen and water without the production of free radicals.

The catalytic mechanism of these enzymes shares many features, as it is depicted in the general scheme of Figure 1. Although the details of the mechanism are not yet fully understood, it is generally accepted that it occurs in two stages.[1,2] In the first stage the heme active center reacts with a molecule of hydrogen peroxide to form compound **I** intermediate. This intermediate has an oxygen atom axially coordinated to the iron and is an Fe(IV)−porphyrin cation radical.[3] Next, a second molecule of hydrogen peroxide becomes oxidized and compound **I** returns to its original state. Alternatively, compound **I** can also react with one electron donors such as aliphatic alcohols and be reduced to compound **II** intermediate, for which the porphyrin has lost the cation radical character. This intermediate may either evolve to compound **III** (which, in the case of catalases, inactivates the enzyme[2,4]) or it may react again with one electron donors and restore the resting state of the enzyme.

The reaction from compound **I** to compound **II** occurs rarely in catalases,[2,4,5] as compound **I** generally reacts with a second molecule of hydrogen peroxide via the so-called *catalatic pathway* (Figure 1). In the catalases of some species, compound **II** has never been detected.[5] On the contrary, peroxidases generally react with hydrogen peroxide via the formation of compounds **I** and **II** (*peroxidatic pathway*).[1b,6]

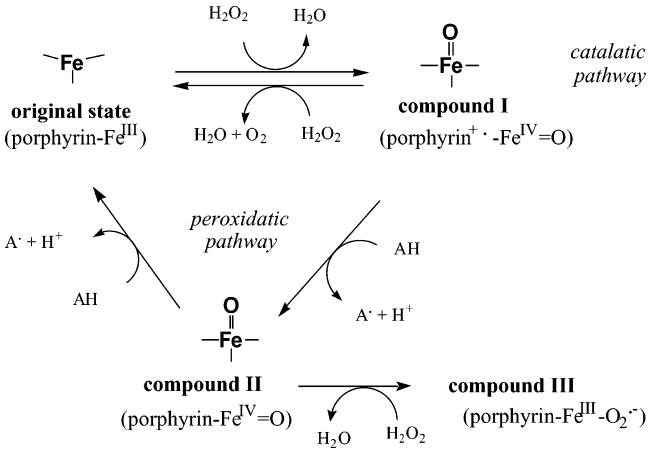

Figure 1. Main reaction scheme of the catalytic cycle of peroxidases and catalases.

This different behavior between peroxidases and catalases may arise from several factors. It could be that kinetic or mechanistic factors favor different reaction paths in the two cases. It could also be that the stability of compound **II** is lower for catalases than for peroxidases.[2] As a matter of fact, catalases have a negatively charged tyrosine axially coordinated to the heme,[1b,2] while peroxidases have a neutral histidine (see Scheme 1). In addition, the tyrosine proximal ligand forms two hydrogen bonds with a conserved arginine residue (positively charged) in catalases,[1b] while the proximal histidine of peroxidases is hydrogen-bonded to a conserved aspartic acid residue (negatively charged).[1d] Therefore, peroxidases and catalases show significant differences not only in the type of proximal residue coordinated to the iron but also in the residues interacting with it.

In this study we will address the question whether the stereochemical properties of the proximal side may affect the

* Corresponding author. E-mail: crovira@pcb.ub.es. Tel: +34 93 4037112. Fax: +34 93 4037225.
† Parc Científic de Barcelona.
‡ Institut de Biologia Molecular de Barcelona.

10.1021/jp0268516 CCC: $25.00
Published on Web 05/13/2003

SCHEME 1

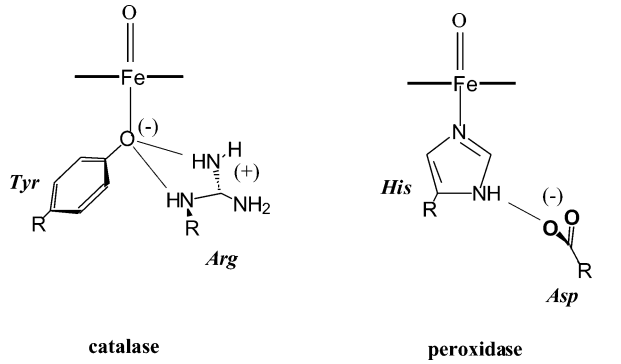

function of the enzyme and, in particular, to the stability of compound **II** intermediate. Our goal is to quantify the changes introduced by the Tyr^-/Arg^+ diad (catalases) with respect to the His/Asp^- pair (peroxidases). We will investigate the structural and energetic properties of compound **II** by means of DFT/molecular dynamics within the Car−Parrinello scheme. This methodology has already been applied with success in studies of other hemeproteins such as myoglobin and cytochrome *c*[7,8]). In addition, DFT has also been used to investigate the compound **I** intermediate of catalases (Figure 1), peroxidases[9] and cytochrome P450.[10] Interestingly, Green demonstrated that the hydrogen-bonded residue of compound **I** changes the localization of the porphyrin radical.[11] Therefore, there is already evidence of the contribution of the hydrogen-bonded residue. Previous investigations have been performed for peroxidase compound **II** at a fixed geometry using models lacking the proximal and/or the hydrogen-bonded residue.[12]

2. Computational Details

Optimization of the molecular structures was performed, with no symmetry constraints, starting from the X-ray structures of *Micrococcus lysodeikticus* catalase[13] and Horseradish peroxidase[14] (PDB entries 1GWE and 1ATJ, respectively). Previous QM/MM calculations on myoglobin[7c] showed that the effect of the protein on the heme-proximal bond structure is not significant. Therefore, the complete protein was not included in the present calculations, keeping only the charged residues close to active center (Arg^+ in catalase and Asp^- in peroxidase, which are not present in myoglobin). On the other hand, this approach allows us to analyze the intrinsic properties of the active center and its interaction with the hydrogen-bonded residue.

The models used for the calculation are shown in Figure 2. The complete heme b group is used with all porphyrin substituents. The axial tyrosine residue of catalase is replaced by a phenolate anion and the hydrogen-bonded arginine by a methylguanidinium cation. Similarly, the proximal histidine residue of peroxidase is replaced by imidazole and the hydrogen-bonded aspartic residue is replaced by a carboxylate anion. It is not expected that such replacements (routinely used in modeling of protein active centers) introduce any bias in the properties investigated. On the other hand, the size of the models used (101 atoms for catalase and 92 for peroxidase) is at the limit of what can be done using first-principles methods. The systems are enclosed in a isolated supercell of sizes $18 \times 17 \times 12$ Å^3 (catalase) and $20 \times 19 \times 15$ Å^3 (peroxidase). The peroxidase compound **II** was computed as neutral, while the catalase compound **II** was computed with a negative charge. With the addition of the hydrogen-bonded residue, the total charge of the complex is −1 for peroxidase and 0 for catalase.

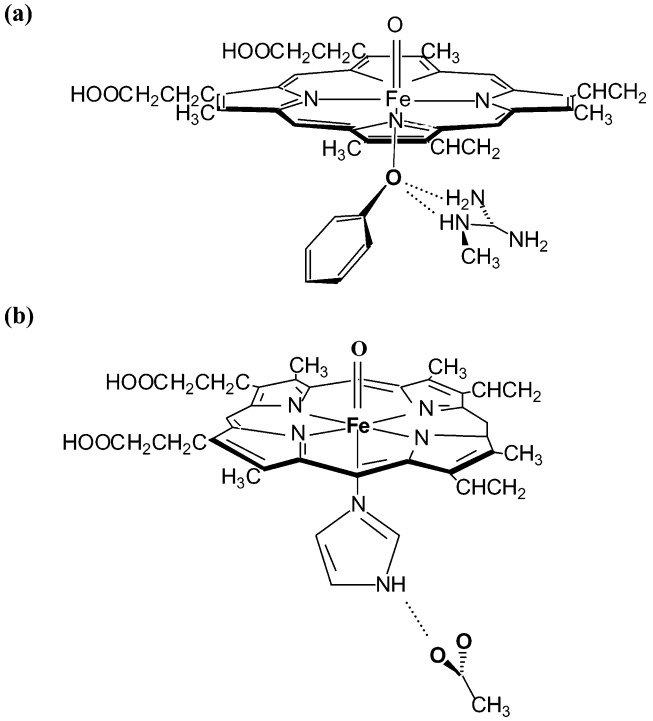

Figure 2. Compound **II** models used in the calculations (see text).

In both cases, the ground state was found to be an Fe(IV) triplet, in agreement with experimental results.[1] The spin density is localized in the Fe═O bond in both cases.

Our calculations were carried out using the Car−Parrinello molecular dynamics method,[15] which is based on DFT. Previous work has demonstrated the reliability of this method in the description of structural, energetic, and dynamical properties of systems of biological interest.[16] The Kohn−Sham orbitals are expanded in a plane wave (PW) basis set with the kinetic energy cutoff of 70 Ry. Earlier calculations on metal−porphyrin models[7a] showed that this cutoff is sufficient for achieving a good convergence of energies and structural properties. We employed ab initio pseudopotentials, generated within the Troullier-Martins scheme,[17] including the nonlinear core correction[18] for the iron atom. Our calculations were made using the generalized gradient-corrected approximation of the spin-dependent density functional theory (DFT-LSD), following the prescription of Becke and Perdew.[19] Structural optimizations were performed by means of molecular dynamics with annealing of the atomic velocities, using a time step of 0.12 fs, and the fictitious mass of the electrons was set at 700 au. Ligand binding energies were computed by subtracting the energy of the optimized isolated fragments from the total energy of the complex. Additional calculations keeping the hydrogen-bonded residues fixed at their position in the protein (relative to the position of the iron-porphyrin) gave very similar results. Because of the use of a PW representation of the electronic density, our optimized structures and computed binding energies are free from the basis set superposition error (BSSE) that affects calculations performed using atom-centered basis set functions.

3. Results and Discussion

3.1. Optimized Structures. The optimized structures of catalase and peroxidase compound **II** are shown in Figure 3. In addition, Table 1 lists the most relevant structural parameters defining each structure, namely the distances and angles involving the Fe−ligand bonds and the hydrogen-bonded

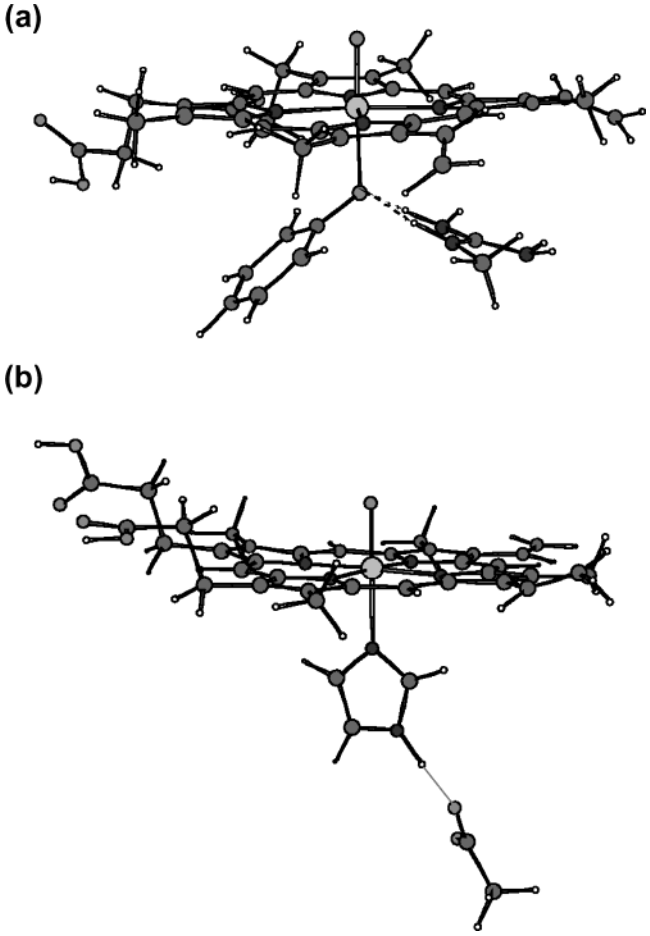

Figure 3. Fully optimized structures corresponding to the compound **II** models. (a) Catalase. (b) Peroxidase.

TABLE 1: Main Structural Parameters Defining the Optimized Structures of the Compound II Models of Figure 2[a]

catalase		peroxidase	
structural parameter	value	structural parameter	value
Fe═O	1.68	Fe═O	1.69
Fe−O	2.12	Fe−N_ϵ	2.09
Fe−N_p	2.01−2.03	Fe−N_p	2.02−2.03
∠O═Fe−O	177.7	∠O═Fe−N_ϵ	179.2
∠Fe−O−C	125.4		
N(arg^+)−H	1.06, 1.07	N_δ−H	1.12
O···H (arg^+)	1.69, 1.76	H···O(asp^-)	1.50

[a] Distances are given in angstroms and angles in degrees.

residues (the complete list of optimized atomic coordinates is given as Supporting Information).

Both catalase and peroxidase compound **II** are stable upon optimization and show similar Fe−ligand bond distances (Table 1). The distance with the proximal ligand is only 0.03 Å shorter for peroxidase (Fe−N_ϵ = 2.09 Å) than that for catalase (Fe−O = 2.12 Å). The hydrogen-bond distance in peroxidase (1.5 Å) is also shorter than any of the two hydrogen bonds of catalase (1.69 and 1.76 Å, see Figure 3), indicating that the hydrogen bond is likely to be stronger in the peroxidase case.

Comparison between our computed structures and the X-ray information available is not straightforward, as very different values have been given for the local structure around the Fe atom. In the case of catalase, there are two X-ray structures available for compound **II**. In the structure of Gouet et al.[20] on *Proteus mirabilis* catalase (PMC) at 2.7 Å resolution (PDB entry 2CAG), both the Fe═O and Fe−O distances are restrained at 1.71 and 1.72 Å, respectively. On the other hand, a recent structure by Murshudov et al. on *Micrococcus lysodeikticus* catalase (MLC) at 1.96 Å resolution (PDB entry 1GWF) gives 1.87 and 2.05 Å, respectively, for these bonds.[13] In the case of peroxidase, two EXAFS measurements for horseradish peroxidase (HRP) have reported very different distances for the Fe═O bond (1.93[21] and 1.64[22] Å, the latter being similar to our computed distance of 1.69 Å). Interestingly, a recent structure on myoglobin compound **II** at 1.35 Å resolution reports an iron−oxygen bond of 1.92 Å, and the authors suggest that it could correspond to an Fe−OH bond instead of Fe═O.[23] The recent high-resolution X-ray structure of HRP gives also a long iron−oxygen bond (1.8 Å), and the authors suggest that a proton has migrated to the ferryl oxygen.[6] In view of all these results and our computed values (1.68−1.69 Å for the Fe═O bond), we support the hypothesis that some of the reported compound **II** structures could contain a hydroxyl group coordinated to the iron atom. In fact, additional calculations on a putative OH-based compound **II** show that it is also a stable intermediate with respect to ligand dissociation, with a much longer Fe−O distance (1.77 Å in both catalase and peroxidase). Therefore, although a more thoughtful investigation of the OH-based intermediate is needed, our results evidence that two type of compound **II** species (oxo and hydroxyl based) might have been trapped by the structural determinations.[24]

TABLE 2: Computed Binding Energies (BE) of the Fe-Axial Bonds[a]

catalase		peroxidase	
bond	BE	bond	BE
Fe═O	−86.3	Fe═O	−108.3
Fe−O	−6.3	Fe−N_ϵ	−31.1

[a] Values in kcal/mol.

Concerning the other Fe−ligand bonds, values in the range 1.72−2.05 Å have been given for the Fe−O(tyr) and 1.86−2.06 Å for the Fe−N_p distances for catalases. The recent high-resolution structure of HRP compound **II** gives an Fe−N_ϵ distance of 2.10 Å,[6] which compares well with our computed value (2.09 Å). Therefore, our computed distances are in the range of values given by structural analyses and, in the case of the Fe═O bond, might help to understand the variability of results that have been reported.

3.2. Ligand Binding Energies. Table 2 lists the computed binding energies of the Fe−ligand bonds in catalase and peroxidase. In both cases, the Fe═O bond is stronger than the Fe-proximal bond (Fe−N_ϵ in peroxidase and Fe−O in catalase). This is expected as most of the electron density of the Fe atom is used in the double bond with the distal oxygen, and as a consequence, there is little density available for the single bond with the proximal residue. The same trend is found in the computed bond orders (1.26 for the Fe═O bond in both catalase and peroxidase and 0.33/0.39 for the Fe−O/Fe−N_ϵ bonds).

In comparison with the results obtained for other hemeproteins, the strength of the Fe(IV)−O proximal bond of catalase is between that of the Fe(II)−N_ϵ bond in myoglobin (−12 kcal/mol)[7a] and that for the Fe−S bond in cytochrome *c* (−7.5 kcal/mol for Fe(II)−S and −3.5 kcal/mol for Fe(III)−S).[8] The results of Table 2 also evidence that the Fe−ligand bonds are stronger for peroxidase comparing to catalase: the strength of the Fe═O and Fe−N_ϵ bonds in peroxidase amounts to −108.3 and −31.1 kcal/mol, respectively, much larger than the values found for catalase (−86.3 and −6.3 kcal/mol, respectively). At first sight, this is surprising since the phenolate residue is expected

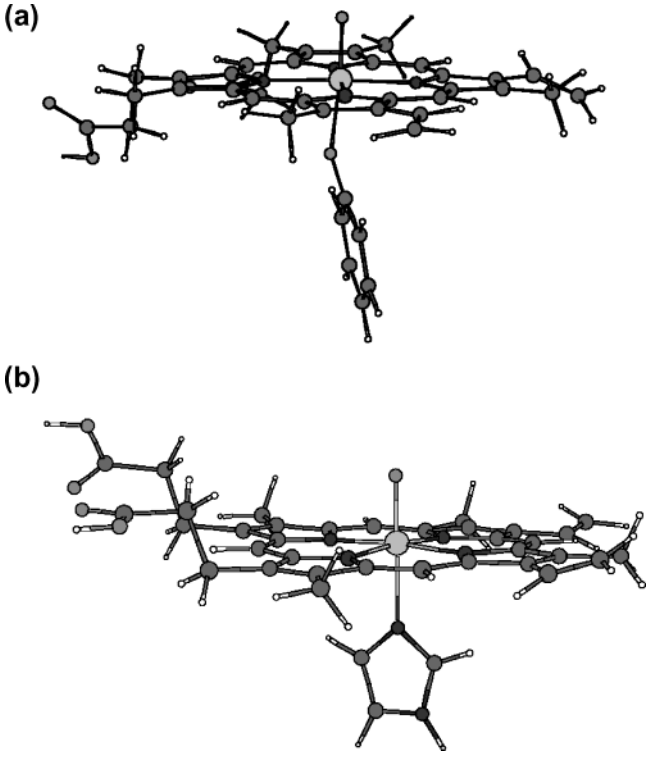

Figure 4. Fully optimized structures corresponding to the compound **II** models, in the absence of the hydrogen-bonded residue. (a) Catalase. (b) Peroxidase.

to be a better donor than the neutral imidazole. A possible explanation is that these differences are partially due to the different orientation of the propionate groups (toward the distal side in peroxidase and toward the proximal side in catalases). However, calculations with the heme upside down in peroxidase gave the same results. Therefore, the stronger binding found in peroxidases comparing to catalases is fully due to the differences in the His/Asp^- pair comparing to the Tyr^-/Arg^+ one. As a matter of fact, it is generally accepted that the aspartate residue gives some degree of imidazolate character to the proximal imidazole in peroxidases.[25] Our calculations show that the effect of the hydrogen-bonded aspartate residue is so strong as to reverse the order of stability of the iron-proximal bond. In the next section, this effect will be quantified.

In summary, we find that the Fe−ligand bonds are significantly stronger for peroxidase comparing to catalase, which can be fully attributed to the effect of the His/Asp^- pair with respect to the Tyr^-/Arg^+ one. This could explain the lower tendency of catalases to give compound **II** compared to peroxidases. However, this could only be part of then reason, as compound **II** is a stable intermediate with respect to ligand dissociation in both cases.

3.3. Role of the Hydrogen-Bonded Residue. As a way to grasp the role of the conserved hydrogen-bonded residue (Arg^+ in catalase and Asp^- in peroxidase), we performed additional calculations removing these residues from the model. Figure 4a shows the optimized structure of catalase compound **II** without the hydrogen-bonded methylguanidinium cation. There is a drastic change in the relative position of the phenolate ligand: the angle between the six-membered ring and the Fe−O bond increases by 31° (see Figures 3a and 4a) The phenolate ligand bends toward the opposite porphyrin quadrant (Fe−O−C = 156°) to minimize the steric repulsion with the heme propionate substituents. There is also a slight tilting of the Fe−O bond with respect to the perpendicular to the porphyrin plane (O═Fe−O = 86°). As a result, the binding energy Fe−O increases from −6.3 (Table 2) to −26.2 kcal/mol. Thus, the methylguanidinium cation weakens the Fe-proximal bond and distorts the position of the phenolate ligand. This situation has some similarities with what was found by Green for catalase compound **I** intermediate,[11] with the exception that no change in the spin density distribution is observed for compound **II**. Moreover, the position of the phenolate group in the complex of Figure 3a is slightly different than what was found for compound I.[26]

Figure 4b shows the optimized structure of peroxidase compound **II** in the absence of the hydrogen-bonded carboxylate anion. In this case, the orientation of the imidazole ligand does not change but the Fe−N_ϵ bond weakens by 23 kcal/mol. At the same time, the Fe atom goes out-of-plane toward the apical oxygen, as if trying to recover the structure of a five-coordinated oxoheme complex, and the Fe−N_ϵ distance enlarges by 0.04 Å. Additional calculations at different Fe−N_ϵ distances show that the energy changes very little with the elongation of the bond, which indicates that the potential with to the Fe−N_ϵ coordinate is relatively shallow.[27]

The reason of the weakening of the bond with the axial imidazole can be inferred by the analysis of the highest energy occupied spin−orbitals. Figure 5 shows the three highest energy spin−orbitals of the peroxidase compound **II** after having removed the hydrogen-bonded carboxylate group. The two unpaired electrons of the system correspond to the Fe(d_{xz}) and Fe(d_{yz}) orbitals in combination with the p orbitals of the apical oxygen (Figure 5a). The next spin−orbital, in decreasing order of energy, is a porphyrin π orbital in antibonding interaction with the lone pair of the imidazole N_ϵ atom (hereafter referred as ϕ_π orbital) (Figure 5b). If we monitor the shape of this orbital during the optimization we observe that as the Fe−imidazole bond increases the weight of the porphyrin nitrogens and that of the imidazole N_ϵ atom decrease. As a result, the antibonding character of ϕ_π disappears (Figure 5b) and its energy shifts down (it becomes the fourth occupied spin−orbital, below that, the d_{xy} orbital of Fe). Therefore, the occupation of ϕ_π desestabilizes the bond with the proximal ligand in peroxidase compound **II** in the absence of the hydrogen-bonded residue. Further evidence for this comes from the results obtained upon removing one electron from the system (i.e. generating the compound **I** intermediate of Figure 1). Analysis of the spin density reveals that an electron has been removed from ϕ_π, and in consequence, the elongation of the Fe−N_ϵ bond is less pronounced.

The situation is different in the presence of the carboxylate group. In this case, the Fe−imidazole bond is stabilized by the change in the sigma donor character of the imidazole. Analysis of the computed charges (Mulliken and ESP charges) on the imidazole before and after addition of the carboxylate group show an increase in the charge on the imidazole. This indicates that the Fe−N_ϵ bond is reinforced by hydrogen bonding with the carboxylate anion. Other hemeproteins with histidine proximal ligands are expected to exhibit a similar behavior upon formation of compound **II**. In the case of myoglobin and hemoglobin, the imidazole of the proximal His is hydrogen-bonded with a neutral peptide oxygen[28] instead of an anionic residue. Thus, stabilization of the Fe−His bond by the hydrogen-bond interaction is also expected, although to a lesser extent. In fact, the axially coordinated imidazole of the myoglobin cavity mutant H93G is little affected by formation of compound **II**.[29] Our calculations predict that the Fe-proximal bond should weaken significantly if the proximal hydrogen-bonded residue is mutated to an apolar residue in compound **II**

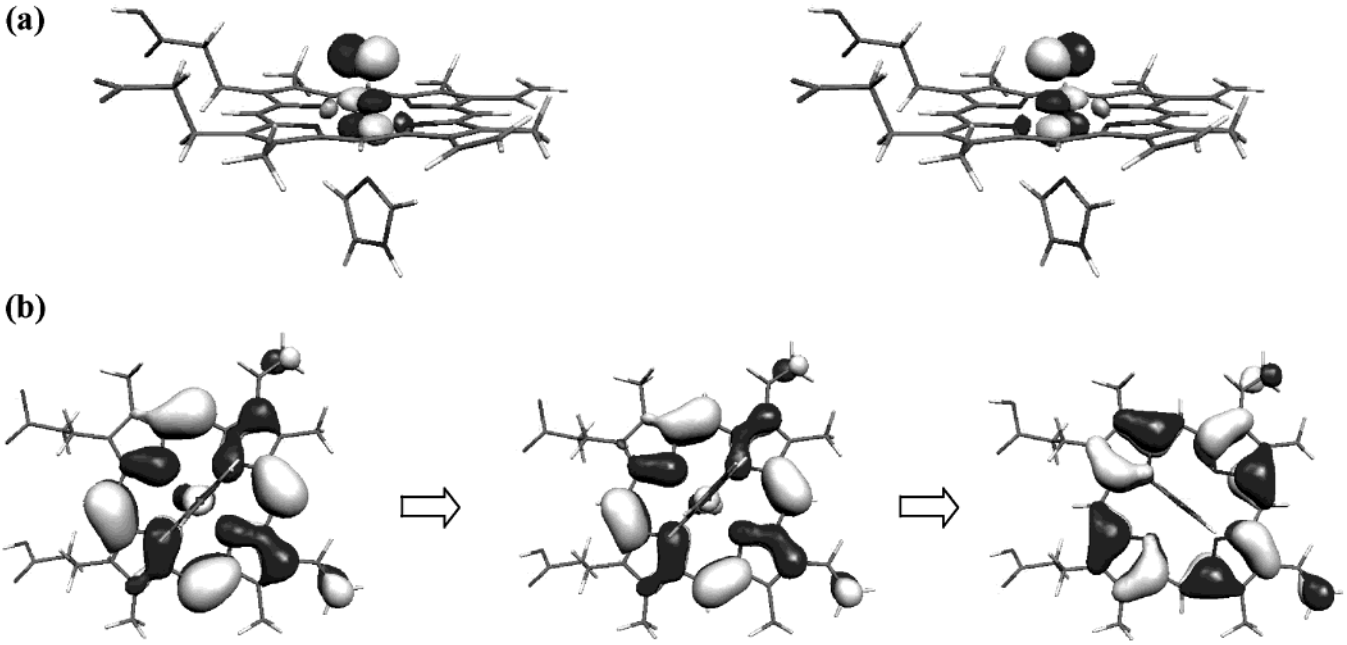

Figure 5. Highest energy occupied spin−orbitals of peroxidase model of Figure 4b, in decreasing order of energy. (a) The two spin−orbitals carrying out the spin density. (b) The third occupied spin−orbital (denoted as ϕ_π in the text). Variation during with elongation of the Fe−N_ϵ bond (Fe−N_ϵ = 2.09 Å in the first picture and 2.46 Å in the last one). The orbital is viewed along the Fe−N_ϵ bond. Only one of the two spin−orbitals is represented.

intermediate. Unfortunately, we are not aware of such type of mutations. However, the D235N mutant of cytochrome *c* peroxidase (Asp→Asn mutation) shows a decrease in the Fe−N_ϵ stretching frequency.[30] Thus, despite the conservative replacement (Asn is also hydrogen-bonded to the imidazole of the proximal His), a weakening of the Fe-proximal bond takes place.

In summary, our calculations reveal that the carboxylate group of the aspartic acid residue is responsible for stabilizing the iron-proximal histidine bond in peroxidase compound **II**. In contrast, the hydrogen-bonded arginine residue of catalase compound **II** weakens the Fe-proximal bond. Therefore, the hydrogen-bonded residues are able to modulate the strength of the Fe-proximal bonds: the energy ordering of the Fe−Tyr^- and Fe−His bonds (Fe-Tyr^- is stronger than Fe−His) is reversed in the presence of the hydrogen-bonded residues (Fe−Tyr^-···Arg^+ is weaker than Fe−His···Asp^-).

4. Conclusions

In this study we have investigated the structural and energetic properties of compound **II** of peroxidases and catalases in order to have some hints concerning the question of why catalases, unlike peroxidases, rarely form compound **II**. In relation to this, the effect of the conserved proximal hydrogen-bonded residue has been quantified.

Our results show that catalase compound **II** is a stable intermediate with respect to ligand disociation, with Fe−ligand binding energies comparable to those found for other heme-proteins, such as myoglobin and cytochrome *c*, using the same methodology. Nevertheless, catalase shows much weaker iron−ligand bonds compared to peroxidase, which could contribute to the lower tendency to form compound **II** compared to peroxidases. Overall, our results do not reveal any indication that compound **II** should not be formed in catalases, as it is found to be stable upon optimization. Therefore, the fact catalases rarely form compound **II** is likely to be due to the kinetics of the catalytic reaction. In this respect, other factors such as steric constraints in the entrance channel for electron donors[31] or the different barriers associated to the steps of the reaction mechanism are likely to play a key role.

The very short Fe−O bonds computed for the compound **II** intermediate (1.68, 1.69 Å for catalase and peroxidase, respectively) compared to values reported in some of the available structural analyses (in particular those giving Fe−O > 1.80 Å) suggests that the latter could correspond to Fe−OH bonds. Therefore, the traditional picture of an oxoferryl compound **II** intermediate should be interpreted with care, as the proton of the electron donor (AH in Figure 1) could migrate to the oxoferryl bond, resulting in a stable intermediate.

Our analysis of the role of the hydrogen-bonded residue reveal striking differences between catalases and peroxidases. In the case of catalases, the hydrogen-bonded residue weakens the Fe-proximal bond, while the opposite occurs in peroxidases. In this case, the Fe−imidazole bond is significantly weaker in the absence of the hydrogen-bonded residue. This could have essential implications for the catalytic reaction of the enzyme, as the hydrogen-bonded residue can control the strength of the Fe-proximal bond and, in turn, the strength of the opposite Fe-axial bond. Therefore, the proximal hydrogen-bonded residue can modulate the stability of the different species coordinated to Fe in the distal side during the catalytic reaction (Figure 1). In this respect, our previous experience in heme−imidazole complexes as models for the active center of myoglobin[7b] demonstrated that the strength of the Fe-proximal bond influences that of the Fe-distal bond. Therefore, changes in the polarity of the residues interacting with the proximal ligand can be transmitted to the distal side of the heme and affect to the stability of the reaction intermediates. To quantify these aspects, an investigation of the catalytic mechanism of hydrogen peroxide decomposition (Figure 1) is needed.[32]

Acknowledgment. We thank Dr. W. R. Melik-Adamyan for sending us his manuscript on the structure catalase compound **II** prior to publication. This work was supported by the CIRIT under project 2001SGR-00044. The computer resources were

provided by the CEPBA-IBM Research Institute of Barcelona. C.R. thanks the financial support from the Ramon y Cajal program of the "Ministerio de Ciencia y Tecnología" (MCYT). We thank one of the referees for very insightful comments on some quantitative aspects of this work.

Supporting Information Available: Fully optimized structures of the complexes investigated. This material is available free of charge via the Internet at http://pubs.acs.org.

References and Notes

(1) (a) Deiseroth, A.; Dounce, A. L. *Physiol. Rev.* **1970**, *50*, 319−375. (b) Nichols, P.; Fita, I.; Loewen, P. C. Enzymology and Structure of Catalases. In *Advances in Inorganic Chemistry*; Sykes, A. G., Mauk, G., Eds.; Academic Press: New York, 2001; Vol. 51, pp 51−106. (c) Dunford, H. B. *Heme Peroxidases*; Wiley: New York, 1999. (d)Veitch, G.; Smith, A. T. Horseradish Peroxidase. In *Advances in Inorganic Chemistry*; Sykes, A. G., Mauk, G., Eds.; Academic Press: New York, 2001; Vol. 51, pp 107−162

(2) Maté, M. J.; Murshudov, G.; Bravo, J.; Melik-Adamyan, W.; Loewen, P. C.; Fita, I. *The Handbook of Metalloproteins*; Messerschmidt, A., Huber, R., Poulos, T., Eds.; John Wiley & Sons: Chichester, 2001; pp 486−502.

(3) Ivancich, A.; Jouve, H. M.; Gaillard, J. *Biochemistry* **1997**, *36*, 9356−9364.

(4) (b) Lardinois, O. M.; Mestdagh, M. M.; Rouxhet, P. *Biochim. Biophys. Acta* **1996**, *1295*, 222−238. (a) DeLuca, D. C.; Dennis, R.; Smith, W. G. *Arch. Biochem. Biophys*. **1995**, *320*, 129−134.

(5) Zámocky, M.; Koller, F. *Prog. Biophys. Mol. Biol*. **1999**, *72*, 19−66.

(6) Berglund, G. I.; Carlsson, G. H.; Smith, A. T.; Szöke, H.; Henriksen, A.; Hajdu, J. *Nature* **2002**, *417*, 463−468.

(7) (a) Rovira, C.; Kunc, K.; Hutter, J.; Ballone, P.; Parrinello. M. *J. Phys. Chem. A* **1997**, *101*, 8914−8925. (b) Rovira, C.; Parrinello. M. *Biophys. J*. **2000**, *78*, 93−100 (c) Rovira, C.; Schulze, B.; Eichinger, M.; Evanseck, J. D.; Parrinello, M. *Biophys. J.* **2001**, *81*, 435−445.

(8) Rovira, C.; Carloni, P.; Parrinello, M. *J. Phys. Chem. B* **1999**, *103*, 7031−7035.

(9) Green, M. T. *J. Am. Chem. Soc.* **1999**, *121*, 7939−7940.

(10) (a) Loew, G.; Dupuis, M. *J. Am. Chem. Soc.* **1996**, *118*, 10584−10587. (b) Wirstam, M.; Blomberg, M. R. A.; Siegbahn, P. E. M. *J. Am. Chem. Soc*. **1999**, *121*, 10178−10185. (c) Green, M. T. *J. Am. Chem. Soc*. **2000**, *122*, 9495−9499. (d) Oligaro, F.; Cohen, S.; Filatov, M.; Harris, N.; Shaik, S. *Angew. Chem., Int. Ed*. **2000**, *39*, 3851−3855. (e) Deeth, R. J. *J. Am. Chem. Soc*. **1999**, *121*, 6074−6075.

(11) Green, M. T. *J. Am. Chem. Soc.* **2001**, *123*, 9218−9219.

(12) (a) Ghosh, A.; Almlöf, J.; Que L., Jr. *J. Phys. Chem*. **1994**, *98*, 5576−5579. (b) Kuramochi, H.; Noodleman, L.; Case, D. A. *J. Am. Chem. Soc.* **1997**, *119*, 11442−11451.

(13) Murshudov, G. N.: Grebenko, J. A.; Branningan, J. A.; Antson, A. A.; Barynin, V. V.; Dodson, G. G.; Dauter, Z.; Wilson, K.; Melik-Adamyan, W. R. *Acta Crystallogr. D.* **2002**, *58*, 1972−1982.

(14) Gajhede, M.; Schuller, D. J.; Henriksen, A.; Smith, A. T.; Poulos, T. L. *Nat. Struct. Biol.* **1997**, *4*, 1032−1038.

(15) (a) Computations were performed using the CPMD 3.0h program. Hutter, J. Max-Planck-Institut für Festkörperforschung: Stuttgart, 1998. (b) Car, R.; Parrinello, M. *Phys. Rev. Lett.* **1985**, *55*, 2471. (c) Galli, G.; Parrinello, M. In *Computer Simulation in Materials Science*; Pontikis, V., Meyer, M., Eds.; Kluwer: Dordrecht, 1991.

(16) For recent reviews on the applications of Car−Parrinello molecular dynamics to biology, see: (a) Carloni, P.; Röthlisberger, U.; Parrinello, M. *Acc. Chem. Res*. In press. (b) Carloni, P.; Röthlisberger, U. Simulations of Enzymatic Systems: Perspectives from Car-Parrinello Molecular Dynamics Simulations. In *Theoretical Biochemistry-Processes and Properties of Biological Systems*; L. Eriksson. L., Ed.; Elsevier Science: New York, 2001; p 215.

(17) Troullier, M.; Martins, J. L. *Phys. Rev. B* **1991**, *43*, 1993.

(18) Louie, S. G.; Froyen, S.; Cohen, M. L. *Phys. Rev. B* **1982**, *26*, 1738.

(19) (a) Becke, A. D. *J. Chem. Phys.* **1986**, *84*, 4524. (b) Perdew, J. P. *Phys. Rev. B* **1986**, *33*, 8822.

(20) Gouet, P.; Jouve, H.-M.; Williams, P. A.; Andersson, I.; Andreoletti, P.; Nussaume, L.; Hajdu, J. *Nat. Struct. Biol.* **1996**, *3*, 951−956.

(21) Chence, B.; Powers, L.; Chiang, Y.; Poulos, T.; Schonbaum, G. R.; Yamazaki, I.; Paul, K. G. *Arch. Biochem. Biophys*. **1984**, *235*, 596−611.

(22) Penner-Hahn, J. E.; Eble, K. S.; McMurry, T. J.; Renner, M.; Balch, A. L.; Groves, J. T.; Dawson, J. H.; Hodgsen, K. O. *J. Am. Chem. Soc.* **1986**, *108*, 7819−7825.

(23) Hersleth, H.-P.; Dalhus, B.; Görbitz, C. H.; Andersson, K. K. *J. Biol. Inorg. Chem.* **2002**, *7*, 299−304.

(24) An investigation of the properties of putative OH-based compound **II** is in progress and the results will be published elsewhere.

(25) Smulevich, G.; Neri, F.; Willemsen, O.; Choudhury, K.; Marzocchi, M. P.; Poulos, T. L. *Biochemistry* **1995**, *34*, 13485−13490.

(26) We do not observe tilting of the phenolate ligand with respect to the perpendicular to the porphyrin plane when viewing it along the perpendicular direction to the benzene ring. Probably the differences in electronic state between compound **I** (ref 11) and compound **II** (this work) are responsible for this variation.

(27) In addition, molecular dynamics simulations at room temperature show a rapid increase of the Fe−N_ϵ bond distance, which is accompanied by an increase of the electronic kinetic energy of the Car−Parrinello lagrangian. This behavior is typical of a system with low-lying excited states. Analyzing in detail the electronic spectrum of this artificial system (the biologically relevant species of Figure 3b do not show this behavior) with respect to the Fe−N_ϵ coordinate would be an interesting exercise to illustrate the influence of the excited-state structure on the dynamics of the system. However, this is out of the scope of the present study.

(28) (a) Poulos, T. L. *J. Biol. Inorg. Chem*. **1996**, *1*, 356−359. (b) Goodin, D. B. *J. Biol. Inorg. Chem.* **1996**, *1*, 360−363.

(29) Roach, M. P.; Ozaki, S. Watanabe, Y. *Biochemistry* **2000**, *39*, 1446−1454.

(30) Wang, J.; Mauro, M.; Edwards, S. L.; Oatley, S. J.; Fishel, L. A.; Ashford, V. A.; Xuong, N.; Kraut, J. *Biochemistry* **1990**, *29*, 7160−7173.

(31) Kalko, S. G.; Gelpí, J. L.; Fita, I.; Orozco, M. *J. Am. Chem. Soc*. **2001**, *123*, 9665−9672.

(32) An investigation of the catalytic reaction path using QM/MM methods is in progress.